Research Square

Preprints are preliminary reports that have not undergone peer review.
They should not be considered conclusive, used to inform clinical practice,
or referenced by the media as validated information.

Multifractal Quantile Detrending Moving-average Cross-correlation Analysis

Sawon Pratiher

sawon1234@gmail.com

Howrah https://orcid.org/0000-0001-8471-8148

Research Article

Keywords:

Posted Date: November 6th, 2026

DOI: https://doi.org/10.21203/rs.3.rs-11631878/v1

License: This work is licensed under a Creative Commons Attribution 4.0 International License.
Read Full License

Additional Declarations: The authors declare no competing interests.

Multifractal quantile detrending moving-average cross-correlation analysis

Sawon Pratiher
Department of Electrical Engineering, Indian Institute of Technology Kharagpur, Kharagpur 721302, West Bengal, India
sawon1234@gmail.com
October 31, 2026

We introduce multifractal quantile detrending moving-average cross-correlation analysis (MF-X-QDMA), the bivariate extension of the quantile detrending moving average algorithm of a jointly submitted companion paper. The local trends of the two profiles are moving quantiles at levels (λ_x, λ_y), in one and two dimensions. For pairs of non-negative measures, the product of the two quantile residuals is exactly a product of gliding-box masses, so MF-X-QDMA measures the joint partition function. This yields the exact cross exponent of two binomial measures, $\tau_{xy}(q) = -\log_2[(p_x p_y)^{q/2} + ((1-p_x)(1-p_y))^{q/2}]$. A Cauchy–Schwarz bound, $\tau_{xy} \geq (\tau_{xx} + \tau_{yy})/2$, shows that the widely used relation $h_{xy} = (h_{xx} + h_{yy})/2$ holds only for identical multipliers. Measured against the exact expression, the error of MF-X-DMA for $(p_x, p_y) = (0.1, 0.45)$ falls from 0.094 to 0.017. For signals, quantile levels $\lambda \neq 1/2$ leave a residual offset that creates spurious cross-correlation (0.44 for independent series at $\lambda = 0.1$); we give three remedies. On benchmarks with known exponents, MF-X-QDMA with mixed levels $(0.1, 0.9)$ is the most accurate estimator for binomial pairs (mean error 0.007, versus 0.012 for MF-X-DMA). In two dimensions it lowers the τ_{xy} error of 256^2 cascade pairs by 27%–35%. For monofractal pairs it is comparable to the best moving-average variant. We apply the method to 16 pairs of daily financial series (stock indices, exchange rates, commodities, VIX, Treasury yields, Bitcoin) and 29 stock–index pairs. Under injected bad ticks, the median-detrended cross-correlation coefficient is less sensitive than the detrending moving-average coefficient for 27–29 of the 29 stock pairs. Combining the median trend with first-order moments roughly halves the sensitivity to gross bad ticks and makes it 3.5–18 times smaller than that of Pearson's coefficient. A rolling analysis recovers the 2001 sign reversal of the stock–bond correlation under errors that distort the Pearson coefficient by 0.27 on average. Quantile detrending does not help against return errors that shift the price level, or against dense microstructure noise.

PACS: 05.40.-a, 05.45.Tp, 89.65.Gh, 89.75.Da

1 Introduction

Detrended cross-correlation analysis [1] and its multifractal generalizations quantify the scale dependence of the joint fluctuations of two nonstationary signals. They include multifractal detrended cross-correlation analysis (MF-DXA, here MF-X-DFA) [2], multifractal detrending moving-average cross-correlation analysis (MF-X-DMA) [3], multifractal cross-correlation analysis (MFCCA) with sign-preserving moments [4], q-dependent detrended correlation coefficients [5], and partial cross-correlations [6]. Scale-resolved correlation coefficients based on detrended covariances, the DCCA and DMCA coefficients [7–9], have become standard tools in finance [10].

All of these methods estimate local trends by least squares. In the companion paper [11] (Paper I) we replaced the moving average of MFDMA [12] by a moving λ-quantile, the local-constant solution of quantile regression [13, 14], and analyzed the resulting univariate method (MFQDMA) in one and two dimensions. Here we develop its bivariate counterpart. Cross-correlation analysis raises questions that do not exist for a single series:

1. the two series can be detrended at different quantile levels;
2. detrended cross-covariances can be negative;
3. a residual offset that is harmless in a variance can create spurious correlation in a covariance;
4. data errors may affect one series, both, or both on the same days.

They also raise a question about the reference values themselves. The relation $h_{xy}(q) = [h_{xx}(q) + h_{yy}(q)]/2$, observed for binomial measures in Ref. [2] and used as the "theoretical" cross exponent in Ref. [3], has not been derived.

Our main results are the following. First, for non-negative measures the product of quantile residuals is exactly a product of gliding-box masses (Proposition 1), so MF-X-QDMA measures the joint partition function. This gives exact cross exponents of binomial and four-multiplier cascade pairs. Together with a Cauchy–Schwarz bound (Proposition 2), it shows that the average rule is exact only for identical multipliers. Second, for signals, quantile levels $\lambda \neq 1/2$ create spurious cross-correlation through a residual offset (Proposition 4); we quantify the effect and give three remedies. Third, numerical benchmarks show three things: mixed levels $(\lambda_x, \lambda_y) = (0.1, 0.9)$ give the most accurate cross exponents of binomial pairs; 2D-MF-X-QDMA is the most accurate estimator for 2D cascade pairs; and low λ helps when outliers hit both series on the same days. Fourth, we apply the method to 16 pairs of daily financial series and 29 stock–index pairs, with real and injected data errors. The median-detrended coefficient, combined with first-order moments, is the least sensitive estimator of scale-resolved correlation under bad ticks. We report as clearly where it does not help.

* Joint submission. This article is the second of two companion papers submitted jointly to Physical Review E. Paper I [11] contains the univariate algorithm in 1D and 2D, its exact properties, the univariate benchmarks, and univariate applications, including a financial study of the same assets. The present paper relies on Paper I for the univariate definitions and results (Sec. 2.1) and does not repeat them; no figure or table is shared between the two papers.

2 The MF-X-QDMA algorithm

2.1 Univariate building block

We use the notation of Paper I [11]. For a series $x(t)$, $t = 1,\dots,N$, the profile is $Y_x(i) = \sum_{t\le i}[x(t) - \langle x\rangle]$ in the signal convention and $Y_x(i) = \sum_{t\le i} x(t)$ in the measure convention. For a window size n and position parameter $\theta \in [0,1]$, the moving λ-quantile is

$$\begin{aligned}\widetilde{Y}_{x,\lambda}(i) &= \mathscr{Q}_\lambda\big\{Y_x(k):\ i - \lceil (n-1)(1-\theta)\rceil \le k \\ &\qquad \le i + \lfloor (n-1)\theta\rfloor\big\},\end{aligned} \tag{1}$$

where $\mathscr{Q}_\lambda$ is the linearly interpolated sample quantile, i.e., the local-constant solution of quantile regression [13, 15]. The residual is $\varepsilon_x(i;\lambda) = Y_x(i) - \widetilde{Y}_{x,\lambda}(i)$. The moving average of MF-X-DMA [3] is the least-squares counterpart. We write $\theta = 0$ (backward windows) unless stated otherwise, as recommended in Paper I.

2.2 One-dimensional MF-X-QDMA

Given two series x and y of equal length and quantile levels (λ_x, λ_y), partition the residual sequences into N_n disjoint segments of size n and compute the segment cross-covariances

$$F^2_\nu(n) = \frac{1}{n}\sum_{i\in\nu}\big[\varepsilon_x(i;\lambda_x) - c_x\big]\big[\varepsilon_y(i;\lambda_y) - c_y\big], \tag{2}$$

where $c_x = c_y = 0$ unless segment centering is used, in which case c_x and c_y are the segment means of the residuals (Sec. 3.3). Two conventions are in use for the qth-order cross fluctuation function. The absolute convention of Refs. [2, 3] is

$$F_{xy,q}(n) = \Big\{\frac{1}{N_n}\sum_{\nu=1}^{N_n}|F^2_\nu(n)|^{q/2}\Big\}^{1/q}. \tag{3}$$

The sign-preserving convention of Ref. [4] is

$$F^{\pm}_{xy,q}(n) = \Big\{\frac{1}{N_n}\sum_{\nu}\mathrm{sign}[F^2_\nu(n)]\,|F^2_\nu(n)|^{q/2}\Big\}^{1/q}, \tag{4}$$

which is defined only where the sum is positive. The cross exponent is defined by the scaling law

$$F_{xy,q}(n) \sim n^{h_{xy}(q)}, \qquad \tau_{xy}(q) = q\,h_{xy}(q) - D_f, \tag{5}$$

with $D_f = 1$ in 1D. For $x = y$ and $\lambda_x = \lambda_y$, Eqs. (2)–(5) reduce to univariate MFQDMA. Unless stated otherwise, we use the absolute convention.

2.3 Scale-resolved correlation coefficients

The detrended cross-correlation coefficient at scale n is

$$\rho_\lambda(n) = \frac{\sum_\nu F^2_{\nu,xy}(n)}{\big[\sum_\nu F^2_{\nu,xx}(n)\sum_\nu F^2_{\nu,yy}(n)\big]^{1/2}}. \tag{6}$$

With moving-average residuals it is the DMCA coefficient [8], the moving-average analog of the DCCA coefficient [7]. The q-dependent generalization of Kwapień *et al.* [5],

$$\rho_{\lambda,q}(n) = \frac{S^{xy}_q(n)}{[S^{xx}_q(n)S^{yy}_q(n)]^{1/2}}, \quad S_q = \frac{1}{N_n}\sum_\nu \mathrm{sign}(F^2_\nu)|F^2_\nu|^{q/2}, \tag{7}$$

reduces to Eq. (6) for $q = 2$. For $q < 2$ it reduces the weight of segments with large fluctuations; for $q > 2$ it increases it. We denote by $\rho_{1/2}$ and $\rho_{1/2,q=1}$ the coefficients obtained with median detrending.

2.4 Two-dimensional MF-X-QDMA

For two fields $X(i_1,i_2)$ and $Y(i_1,i_2)$, the 2D residual fields ε_X and ε_Y are computed as in Sec. II C of Paper I: box sums minus the λ-quantile of the within-window partial sums. The box cross-covariances are $F^2_{\nu_1\nu_2}(n) = n^{-2}\sum\varepsilon_X\varepsilon_Y$ over disjoint $n\times n$ boxes. Equations (3)–(5) then apply with $D_f = 2$.

3 Exact properties

3.1 Measures: joint partition function

Proposition 1 (Cross gliding-box representation)**.** *Let $x, y \ge 0$ be analyzed in the measure convention with the same θ. Then*

$$\varepsilon_x(i;\lambda_x)\,\varepsilon_y(i;\lambda_y) = \mu_x\big((i-\ell_x, i]\big)\,\mu_y\big((i-\ell_y, i]\big), \tag{8}$$

with $\ell = \lceil (n-1)(1-\theta)\rceil - \lambda(n-1)$ for each series. For $\lambda_x = \lambda_y$, the segment cross-covariance F^2_ν is the mean of $\mu_x(B)\mu_y(B)$ over the gliding boxes B of length ℓ ending in segment ν.

Proof. Apply Proposition 1 of Paper I to each factor. □

Following the argument of Corollary 2 of Paper I, $F^q_{xy,q}(n) \propto (n/N)\sum_\nu[\mu_x\mu_y](cn)^{q/2}$ with $c = |1-\theta-\lambda|$. Define the joint partition function $Z_{xy}(q,s) = \sum_B[\mu_x(B)\mu_y(B)]^{q/2} \sim (s/N)^{\tau_{xy}(q)}$ over a partition into boxes of size s. Then

$$h_{xy}(q) = \frac{\tau_{xy}(q)+1}{q}. \tag{9}$$

For $\lambda_x \ne \lambda_y$ the two boxes in Eq. (8) are nested, with lengths $c_x n$ and $c_y n$. Both scale with n, so the exponent is asymptotically the same.

Corollary 1 (Exact cross exponents of cascade pairs)**.** *For two binomial measures with multipliers $(p_x, 1-p_x)$ and $(p_y, 1-p_y)$ assigned to the same halves at every iteration [2, 3],*

$$\tau_{xy}(q) = -\log_2\big[(p_xp_y)^{q/2} + ((1-p_x)(1-p_y))^{q/2}\big], \tag{10}$$

$$h_{xy}(0) = -\frac{\ln p_x + \ln(1-p_x) + \ln p_y + \ln(1-p_y)}{4\ln 2}. \tag{11}$$

For two four-multiplier 2D cascades with multipliers $\{p_i\}$ and $\{p'_i\}$ on the same quadrants, $\tau_{xy}(q) = -\log_2\sum_{i=1}^4(p_ip'_i)^{q/2}$ and $h_{xy} = (\tau_{xy}+2)/q$.

Proof. A box at level k with a "left" choices has $\mu_x\mu_y = (p_xp_y)^a[(1-p_x)(1-p_y)]^{k-a}$, so $Z_{xy} = [(p_xp_y)^{q/2} + ((1-p_x)(1-p_y))^{q/2}]^k$ by the binomial theorem. Equation (11) follows from L'Hôpital's rule, as in Paper I. The 2D case is identical with four terms. □

Proposition 2 (Cauchy–Schwarz bound)**.** *For any two measures on a common partition and all q,*

$$\tau_{xy}(q) \;\geq\; \frac{\tau_{xx}(q)+\tau_{yy}(q)}{2}. \tag{12}$$

Hence $h_{xy}(q) \geq [h_{xx}(q)+h_{yy}(q)]/2$ for $q>0$ and $\leq$ for $q<0$. Equality for all q holds if and only if $\mu_x \propto \mu_y$ on every box. For the binomial pair this means $p_x = p_y$.

Proof. $Z_{xy} = \sum_B \mu_x^{q/2}\mu_y^{q/2} \leq (\sum_B \mu_x^q)^{1/2}(\sum_B \mu_y^q)^{1/2} = (Z_{xx}Z_{yy})^{1/2}$. Taking $-\log$ and dividing by $\log(N/s)$ gives Eq. (12). □

The average rule $h_{xy} = (h_{xx}+h_{yy})/2$ is therefore the equality case of a general inequality. For the pair $(0.3, 0.4)$ of Refs. [2, 3], the two expressions differ by at most 0.013. This is below the resolution of those studies and explains why the rule appeared to hold. For $(0.1, 0.45)$ the difference reaches 0.14 (Sec. 4.1). The average rule remains exact for bivariate fractional Brownian motion [16], whose cross exponent is $H_{xy} = (H_{xx}+H_{yy})/2$, and we use it there.

Corollary 2 (Degeneracy)**.** *By Corollary 1 of Paper I, MF-X-QDMA of measures degenerates if $|\ell_x| < 1$ or $|\ell_y| < 1$, i.e., if $\theta+\lambda_x = 1$ or $\theta+\lambda_y = 1$. This includes the centered median, $\theta = \lambda_x = \lambda_y = 1/2$.*

3.2 Signals: equivariance, reflection, and sign

Proposition 3 (Equivariance)**.** *In the signal convention, let $x' = ax+b$ and $y' = cy+d$ with $ac \neq 0$. Define $\lambda^* = \lambda$ if the coefficient of the series is positive and $\lambda^* = 1-\lambda$ otherwise. Then*

$$F_\nu^2(n;\lambda_x,\lambda_y;x',y') = ac\,F_\nu^2(n;\lambda_x^*,\lambda_y^*;x,y). \tag{13}$$

Consequently, h_{xy} in the absolute convention is invariant up to the exchange $\lambda \to 1-\lambda$ of a reflected series. In contrast, $\rho_\lambda(n)$, $\rho_{\lambda,q}(n)$, and $F^{\pm}_{xy,q}$ change sign if $ac<0$.

The proof follows from Proposition 2 of Paper I applied to each residual. Two practical consequences follow. First, an anticorrelated pair, such as the S&P 500 and the VIX in Sec. 5, can be analyzed in the sign-preserving convention by replacing y with $-y$ and λ_y with $1-\lambda_y$. Second, the absolute convention does not distinguish correlation from anticorrelation; the sign must be read from $\rho_\lambda(n)$.

3.3 Offset-induced spurious cross-correlation

In the univariate case, the residual of a quantile trend at $\lambda \neq 1/2$ has a nonzero mean, $m(n,\lambda) = \langle \varepsilon(i;\lambda)\rangle$. For example, a low quantile trend lies below the profile on average, so $m > 0$. In a variance this offset merely rescales F_q (Paper I). In a covariance it does not cancel.

Proposition 4 (Offset bias)**.** *Let x and y be independent signals with residual offsets $m_x(n,\lambda_x)$ and $m_y(n,\lambda_y)$ and residual variances $\sigma_x^2(n)$ and $\sigma_y^2(n)$. Without centering,*

$$\langle \rho_\lambda(n)\rangle \simeq \frac{m_x m_y}{[(\sigma_x^2+m_x^2)(\sigma_y^2+m_y^2)]^{1/2}} \neq 0. \tag{14}$$

For processes with symmetric increments, the reflection identity of Paper I gives $m(n,1-\lambda) = -m(n,\lambda)$ and $m(n,1/2) = 0$. Equal levels $\lambda_x = \lambda_y \neq 1/2$ therefore produce spurious positive correlation, and complementary levels $(\lambda, 1-\lambda)$ produce spurious negative correlation.

Three remedies remove the bias:

1. use the median, $\lambda = 1/2$;
2. use the midhinge trend $[\mathcal{Q}_\lambda + \mathcal{Q}_{1-\lambda}]/2$, for which the offsets cancel by reflection;
3. center the residuals within each segment ($c_{x,y}$ in Eq. (2)).

Centering is not applied in the measure convention, where the residuals are box masses (Proposition 1) and their mean is part of the signal. Table 1 and Fig. 1 quantify the effect for bivariate fractional Gaussian noise (BFGN) with known ρ. For independent series, raw $\lambda = 0.1$ gives $\hat\rho = +0.36$ to $+0.44$ and raw $(0.1, 0.9)$ gives -0.33 to -0.44, whereas all three remedies give $|\hat\rho| \leq 0.02$. A remaining effect is attenuation. Quantile residuals are nonlinear functions of the data, so their correlation is somewhat smaller than ρ: $\hat\rho/\rho = 0.87$–0.99 for centered $\lambda \leq 0.25$, against 0.96–1.00 for $\lambda = 1/2$ and the moving average. Because of this attenuation, the median is the natural choice for estimating correlation coefficients.

4 Numerical experiments

4.1 Binomial-measure pairs

We generate eight binomial pairs ($N = 2^{16}$) with a common split pattern, from identical multipliers $(0.3, 0.3)$ to strongly different ones $(0.1, 0.45)$. We analyze them in the measure convention with $16 \leq n \leq 2048$ (14 scales) and $q \in [-4, 4]$, and compare $h_{xy}(q)$ with Eq. (10) and with the average rule (Table 2, Fig. 2).

Two results stand out. First, the exact expression is correct and the average rule is not. For the backward MF-X-DMA, the RMSE with respect to the average rule grows with the gap between the two formulas, up to 0.094 for $(0.1, 0.45)$. Measured against Eq. (10), it stays at 0.004–0.024 for all pairs [Fig. 2(b)]. All moving-window estimators follow the exact curve [Fig. 2(a)]. Second, MF-X-QDMA with mixed levels $(\lambda_x, \lambda_y) = (0.1, 0.9)$ is the most accurate estimator for all eight pairs. Its mean RMSE is 0.007, against 0.012 for backward MF-X-DMA, 0.013–0.015 for equal levels, and 0.060 for MF-X-DFA. With equal levels, MF-X-QDMA ties MF-X-DMA, as in the univariate case (Paper I). The mixed configuration pairs a long box for x with a short box for y [Eq. (8)]. We observe its advantage empirically and do not have a theoretical explanation. The centered median is degenerate (mean RMSE

Table 1: Mean detrended cross-correlation coefficient $\hat{\rho}$ (average over 10 scales $10 \le n \le 500$ and six realizations, $N = 2^{14}$) of BFGN pairs with equal Hurst exponents H and correlation ρ. "Raw" quantile residuals carry the offset of Proposition 4.

	$H = 0.4$				$H = 0.7$			
Trend	$\rho = 0$	0.3	0.6	0.9	$\rho = 0$	0.3	0.6	0.9
Moving mean (DMCA)	-0.00	+0.30	+0.60	+0.90	+0.01	+0.30	+0.60	+0.90
$\lambda = 1/2$	-0.00	+0.29	+0.59	+0.89	+0.00	+0.30	+0.59	+0.89
$\lambda = 0.25$, raw	+0.20	+0.43	+0.67	+0.91	+0.18	+0.41	+0.65	+0.91
$\lambda = 0.25$, centred	-0.01	+0.28	+0.58	+0.89	-0.00	+0.27	+0.56	+0.88
$\lambda = 0.1$, raw	+0.44	+0.60	+0.76	+0.94	+0.36	+0.53	+0.72	+0.92
$\lambda = 0.1$, centred	-0.01	+0.27	+0.57	+0.88	+0.01	+0.26	+0.54	+0.87
$(0.1, 0.9)$, raw	-0.44	-0.30	-0.16	-0.04	-0.33	-0.19	-0.05	+0.08
$(0.1, 0.9)$, centred	-0.01	+0.25	+0.50	+0.74	-0.01	+0.21	+0.41	+0.59

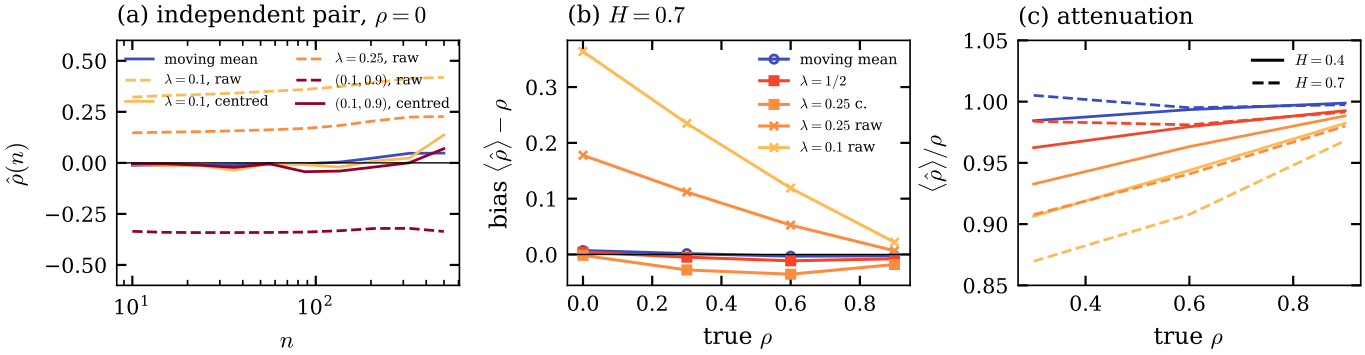


Figure 1: Offset-induced spurious cross-correlation (Proposition 4). (a) $\hat{\rho}(n)$ of independent BFGN pairs ($H = 0.7$, mean of six realizations) for raw and segment-centered quantile residuals. (b) Bias $\langle\hat{\rho}\rangle - \rho$ versus the true ρ ($H = 0.7$). (c) Attenuation $\langle\hat{\rho}\rangle/\rho$ of the unbiased estimators for $H = 0.4$ (solid) and $H = 0.7$ (dashed); colors as in (b).

0.92), as predicted by Corollary 2. The centered moving average (0.053) and MF-X-DFA are the least accurate methods for measures, in agreement with Refs. [3, 12].

4.2 Two-dimensional cascade pairs

Pairs of the four-multiplier cascades A, B, and C of Paper I (256×256, same quadrant assignment) are analyzed with 2D-MF-X-DMA and 2D-MF-X-QDMA ($6 \le n \le 32$, backward windows, measure convention). As Table 3 and Fig. 3 show, the exact τ_{xy} of Corollary 1 fits better than the average rule for every pair and every estimator. 2D-MF-X-QDMA with $\lambda = 0.25$ is the most accurate estimator for all three pairs, lowering the error of 2D-MF-X-DMA by 27% (A–B), 29% (A–C), and 35% (B–C). This mirrors the univariate 2D result of Paper I. In 2D, the quantile of the n^2 within-window partial sums is not reducible to a single box (Paper I, Sec. V A), and it is a genuinely different trend functional.

4.3 Monofractal pairs

We use the 75 BFGN pairs ($N = 2^{15}$; $H_{xx}, H_{yy} \in \{0.1, 0.3, 0.5, 0.7, 0.9\}$; $\rho \in \{0.1, 0.5, 0.9\}$) and the 26 two-component ARFIMA pairs with $d_1 = d_2$ of the corpus of Paper I. The ARFIMA processes are generated by exact circulant embedding [17–19], following Ref. [3]; the theoretical cross exponents are $H_{xy} = (H_{xx} + H_{yy})/2$ and $H = 1/2 + d$, respectively. As Table 4 and Fig. 4 show, the centered MF-X-DMA is the most accurate estimator for both families, as reported in Ref. [3]. MF-X-QDMA with $\lambda = 1/2$ comes second for ARFIMA and third for BFGN. It improves on the backward MF-X-DMA by 13% for BFGN and 15% for ARFIMA. For the correlation coefficient, all estimators are within 0.04 of the nominal ρ of BFGN pairs with $H_{xx} = H_{yy}$. The quantile estimators show the attenuation discussed in Sec. 3.3 [Fig. 4(c)].

4.4 Contaminated pairs

* Binomial pair. We contaminate the $(0.3, 0.4)$ pair by replacing a fraction ε of values with $\pm 20\sigma$ outliers in three ways: in x only, in both series on independent days, and in both series on common days, which mimics a market-wide data error. Table 5 and Figs. 5(a)–5(c) show the results. The clean errors are 0.004 (MF-X-DMA) and 0.004–0.008 (MF-X-QDMA). The benefit of the quantile trend depends on the error structure:

- *Common days*: low levels are the most robust for every $\varepsilon \ge 2\%$. With $\lambda = 0.1$ the error of MF-X-DMA is lower by 39%, 49%, and 40% at $\varepsilon = 2$, 5, and 10%.
- *Errors in x only*: $\lambda = 0.25$ is best at 2% and 5% (0.065 and 0.086, versus 0.071 and 0.122 for MF-X-DMA).
- *Independent errors in both*: $\lambda = 0.25$ is best at 5% (0.088 versus 0.109), and $\lambda = 0.1$ at 10% (0.121 versus 0.231).

At small ε, $\lambda = 0.1$ can be worse than MF-X-DMA, and $\lambda = 0.9$ is among the worst estimators throughout, as in Paper I.

Table 2: Binomial-measure pairs ($N = 2^{16}$): RMSE of $h_{xy}(q)$, $q \in [-4,4]$. "Gap" is $\max_q |h_{xy}^{\text{exact}} - h_{xy}^{\text{avg}}|$. The second column is MF-X-DMA measured against the average rule; all other columns are measured against the exact Eq. (10). Backward windows; bold: best per row.

		MF-X-DMA	MF-X-DMA	MF-X-DFA		MF-X-QDMA	
(p_x, p_y)	Gap	vs average	vs exact	vs exact	$\lambda = 0.25$	$\lambda = 0.5$	$(\lambda_x, \lambda_y) = (0.1, 0.9)$
(0.3, 0.3)	0.000	0.008	0.008	0.045	0.010	0.012	**0.005**
(0.25, 0.35)	0.011	0.006	0.008	0.047	0.010	0.012	**0.004**
(0.3, 0.4)	0.013	0.007	**0.004**	0.043	0.005	0.008	**0.004**
(0.2, 0.3)	0.010	0.012	0.015	0.057	0.017	0.018	**0.008**
(0.2, 0.45)	0.072	0.054	0.007	0.060	0.008	0.011	**0.003**
(0.15, 0.4)	0.067	0.043	0.013	0.064	0.015	0.016	**0.006**
(0.1, 0.3)	0.049	0.027	0.024	0.079	0.026	0.025	**0.016**
(0.1, 0.45)	0.137	0.094	0.017	0.088	0.018	0.018	**0.011**
Mean	—	0.031	0.012	0.060	0.013	0.015	**0.007**

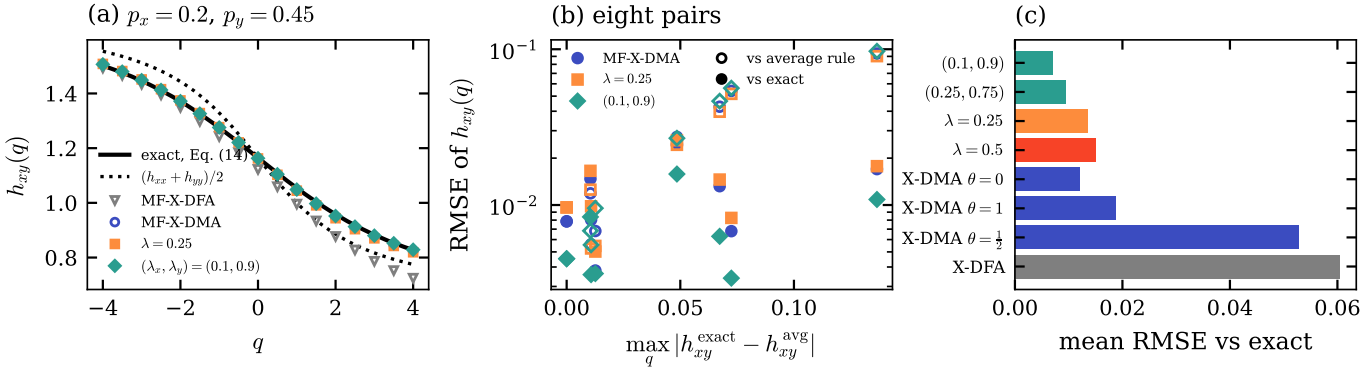


Figure 2: Binomial-measure pairs. (a) $h_{xy}(q)$ for $(p_x, p_y) = (0.2, 0.45)$: exact joint-partition result [Eq. (10)], average rule (dotted), and four estimators. (b) RMSE of h_{xy} against the average rule (open symbols) and against the exact result (filled) versus the gap between the two, for eight pairs. (c) Mean RMSE against the exact result over the eight pairs.

Table 3: 2D cascade pairs (256×256): RMSE of $\tau_{xy}(q)$ against the average rule / against the exact result. Bold: best per row.

Pair	Gap	Mean	$\lambda = 0.25$	$\lambda = 0.5$	$\lambda = 0.75$
A–B	0.085	0.293/0.256	0.226/**0.187**	0.264/0.226	0.367/0.334
A–C	0.051	0.281/0.274	0.205/**0.194**	0.242/0.233	0.344/0.339
B–C	0.147	0.219/0.204	0.168/**0.133**	0.195/0.173	0.280/0.276

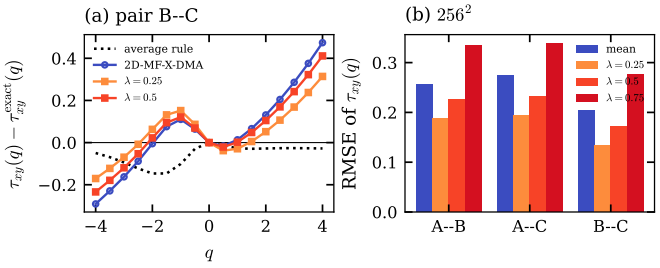


Figure 3: 2D cascade pairs. (a) Deviation of $\tau_{xy}(q)$ from the exact result for the pair B–C; the dotted line is the average rule. (b) RMSE of τ_{xy} against the exact result for three pairs and four trend functionals.

* BFGN pairs. For signals the relevant errors are *spikes* (a single erroneous increment, which shifts the profile permanently) and *bad ticks* (a pair of increments $+s, -s$, which displaces a single profile value). We inject 10σ errors at 0.5%–5% of the samples of BFGN pairs ($H = 0.6/0.6$ and $0.4/0.8$, $\rho = 0.6$, two realizations each). We then measure the change D_h of $h_{xy}(q)$ for $q \in [1,4]$ and the change of $\rho(n)$, each relative to the same estimator on clean data [Fig. 5(d)]. The results anticipate those of the financial data (Sec. 5.3).

- *Bad ticks, coefficient.* The median-detrended coefficient $\rho_{1/2}$ is less sensitive than the DMCA coefficient in all 48 configurations of each mode (median ratio 0.94). Its first-order version $\rho_{1/2,q=1}$ has 0.66–0.67 times the sensitivity of the DMCA coefficient.

- *Spikes, coefficient.* Spikes shift the profile permanently, and no variant improves on the moving average (ratio 1.00–1.05), as expected from Paper I.

- *Centering.* The centered $\lambda = 0.25$ coefficient is the most sensitive estimator for both kinds of errors.

- *Cross exponents.* For $h_{xy}(q \in [1,4])$, the moving average is slightly less sensitive than the quantile trends for 10σ bad ticks. On clean data, $\lambda = 1/2$ is slightly more accurate for $q > 0$ (RMSE 0.018 and 0.024, versus 0.020 and 0.027 for MF-X-DMA).

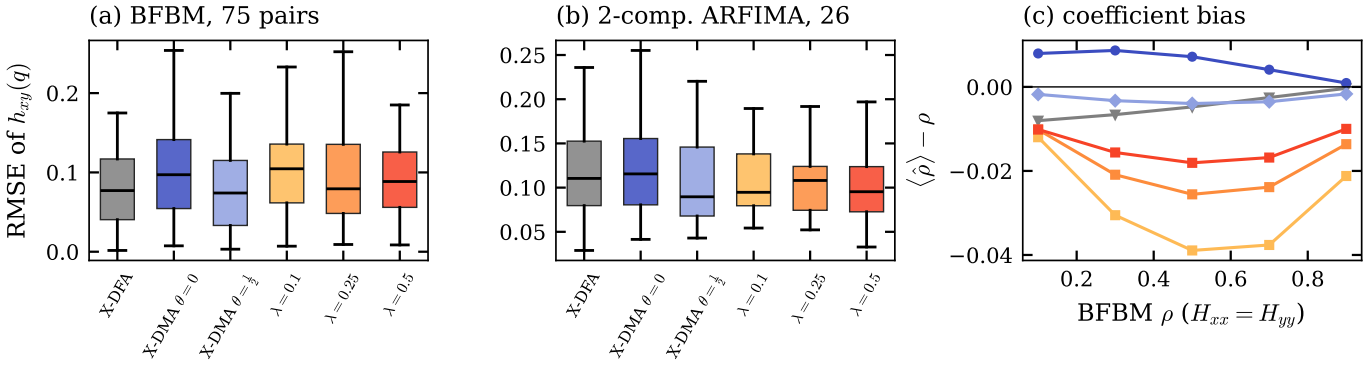


Figure 4: Monofractal pairs. (a) RMSE of $h_{xy}(q)$ for 75 BFGN pairs and (b) for 26 two-component ARFIMA pairs (boxes: quartiles; whiskers: 5%–95%). (c) Bias of the mean detrended coefficient for BFGN pairs with $H_{xx} = H_{yy}$ versus the nominal ρ.

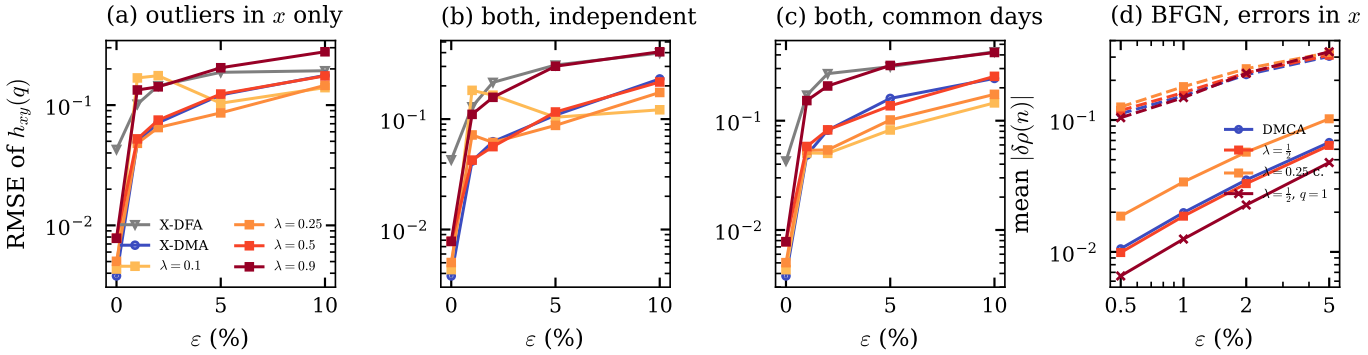


Figure 5: Contaminated pairs. (a)–(c) RMSE of $h_{xy}(q)$ of the binomial pair $(0.3, 0.4)$ versus the fraction ε of $\pm 20\sigma$ outliers, for errors in x only, in both series on independent days, and in both on common days. (d) BFGN pairs: change of the detrended coefficient, mean over scales, for bad ticks (solid) and spikes (dashed) in x only.

Table 4: Monofractal pairs: RMSE (mean $\pm$ s.d.) of $h_{xy}(q)$. Backward windows except where noted; quantile residuals segment-centered (signal convention). Bold: best per column.

Method	BFGN (75)	ARFIMA (26)
MF-X-DFA	0.079 ± 0.048	0.119 ± 0.053
MF-X-DMA, $\theta = 0$	0.103 ± 0.062	0.127 ± 0.063
MF-X-DMA, $\theta = 1/2$	$\mathbf{0.078 \pm 0.052}$	$\mathbf{0.107 \pm 0.050}$
MF-X-DMA, $\theta = 1$	—	0.114 ± 0.045
MF-X-QDMA, $\lambda = 0.1$	0.106 ± 0.059	0.113 ± 0.043
MF-X-QDMA, $\lambda = 0.25$	0.096 ± 0.061	0.109 ± 0.045
MF-X-QDMA, $\lambda = 0.5$	0.089 ± 0.044	0.108 ± 0.054

5 Financial cross-correlations

5.1 Data

We analyze 16 pairs of daily series from the `qrmdata` collection [20, 21], whose univariate properties are analyzed in Paper I (Table 6). The pairs are:

- *Stock indices in the same market*: S&P 500–DJIA, and DJIA–NASDAQ-100, the pair of Ref. [3].
- *Cross-market stock indices*: S&P 500–FTSE, DAX–CAC, FTSE–DAX, Nikkei–Hang Seng, Hang Seng–SSE Composite, and SSE Composite–CSI 300.
- *Exchange rates against the dollar*: EUR–GBP and EUR–JPY.
- *Cross-asset*: gold–EUR, gold–Brent oil, S&P 500–VIX (log changes), and S&P 500–10-year Treasury yield.
- *Interest rates*: 2-year–10-year Treasury yields (daily changes of the Fed zero-coupon curve [22]).
- *Cryptocurrency*: Bitcoin–S&P 500.

Prices are aligned on common trading days, and increments are computed on the common calendar. In addition, we pair each of the 29 DJIA constituents with the DJIA index (2000–2015, $N = 4023$). We use the signal convention, backward windows, $10 \le n \le \min(500, N/10)$ days, and $q \in [-4, 4]$.

5.2 Correlations across scales and cross-exponents

Figure 6 and Table 6 summarize the clean analysis. Five features are relevant for the estimator comparison that follows.

(i) *Scale dependence.* For markets that close at different times, the daily Pearson coefficient underestimates the co-movement: S&P 500–FTSE has $r = 0.49$, but $\rho_{1/2}(n)$ rises from 0.67 at $n = 10$ days to about 0.9 at $n \approx 300$ days [Fig. 6(c)]. This is the nonsynchronous-trading analog of

Table 5: Contaminated binomial pair $(0.3, 0.4)$: RMSE of $h_{xy}(q)$ against Eq. (10), mean of five replicates, for $\pm 20\sigma$ outliers in a fraction ε of values. Backward windows; bold: best per column.

	x only			Both, independent days			Both, common days		
Method	2%	5%	10%	2%	5%	10%	2%	5%	10%
MF-X-DFA	0.145	0.187	0.193	0.215	0.309	0.397	0.270	0.312	0.427
MF-X-DMA	0.071	0.122	0.177	0.062	0.109	0.231	0.082	0.160	0.244
$\lambda = 0.1$	0.176	0.104	**0.140**	0.165	0.104	**0.121**	**0.050**	**0.082**	**0.146**
$\lambda = 0.25$	**0.065**	**0.086**	0.146	0.061	**0.088**	0.174	0.054	0.101	0.174
$\lambda = 0.5$	0.075	0.124	0.175	**0.056**	0.116	0.217	0.082	0.137	0.255
$\lambda = 0.9$	0.142	0.204	0.278	0.158	0.301	0.407	0.208	0.320	0.421

Table 6: Sixteen daily financial pairs: period, length N, Pearson coefficient r, mean detrended coefficients over scales (DMCA ρ, median-detrended $\rho_{1/2}$, and its first-order version $\rho_{1/2,q=1}$), and $h_{xy}(2)$ of returns and of absolute returns for MF-X-DMA and MF-X-QDMA ($\lambda = 1/2$). Data from Ref. [20].

							$h_{xy}(2)$, returns		$h_{xy}(2)$, |returns|	
Pair	Period	N	r	ρ	$\rho_{1/2}$	$\rho_{1/2,q=1}$	X-DMA	$\lambda = \frac{1}{2}$	X-DMA	$\lambda = \frac{1}{2}$
S&P 500–DJIA	1985–15	7796	+0.97	+0.96	+0.95	+0.96	0.51	0.51	0.87	0.96
DJIA–NDX	1985–15	7627	+0.73	+0.73	+0.73	+0.80	0.52	0.48	0.88	0.97
S&P 500–FTSE	1984–15	8060	+0.49	+0.82	+0.82	+0.83	0.54	0.53	0.89	1.04
DAX–CAC	1990–15	6302	+0.84	+0.90	+0.90	+0.92	0.55	0.55	0.88	1.02
FTSE–DAX	1990–15	6348	+0.76	+0.81	+0.80	+0.83	0.54	0.51	0.89	1.02
Nikkei–HSI	1987–15	6833	+0.47	+0.44	+0.43	+0.47	0.53	0.54	0.84	0.95
HSI–SSEC	1990–15	6132	+0.17	+0.31	+0.30	+0.39	0.57	0.59	0.91	1.01
SSEC–CSI 300	2005–15	2612	+0.98	+0.98	+0.98	+0.99	0.67	0.64	0.89	0.85
EUR–GBP	2000–15	4173	+0.66	+0.72	+0.71	+0.82	0.55	0.57	0.91	1.01
EUR–JPY	2000–15	4173	+0.26	+0.28	+0.27	+0.35	0.53	0.53	0.87	0.95
Gold–EUR	2000–15	4173	+0.30	+0.40	+0.40	+0.48	0.49	0.46	0.89	0.99
Gold–Brent	1987–15	7257	+0.17	+0.26	+0.25	+0.31	0.50	0.49	0.91	0.99
S&P 500–VIX	1990–15	6552	-0.71	-0.61	-0.61	-0.67	0.39	0.36	0.81	0.84
UST 2y–UST 10y	1985–15	7508	+0.78	+0.74	+0.72	+0.82	0.50	0.53	0.85	0.78
S&P 500–UST 10y	1985–15	7499	+0.07	+0.08	+0.08	+0.07	0.45	0.48	0.89	0.95
Bitcoin–S&P 500	2010–15	1375	+0.03	+0.19	+0.19	+0.35	0.50	0.54	0.87	0.84

the Epps effect [23]. For markets that trade simultaneously (DAX–CAC, UST 2y–10y), $\rho(n)$ stays within about 0.1 of r up to $n \approx 100$ days.

(ii) *Anticorrelation.* The S&P 500 and the VIX are strongly anticorrelated ($r = -0.71$, $\rho_{1/2} \approx -0.61$), the leverage-type relation behind the "fear gauge" [24]. The absolute convention, Eq. (3), gives a well-defined $h_{xy}(q)$; the sign is carried by $\rho(n)$ (Proposition 3).

(iii) *Sign changes.* The S&P 500–10-year Treasury correlation is near zero over 1985–2015 ($r = 0.07$) because it reverses sign around 2000 [25] (Sec. 5.4).

(iv) *Cross-exponents.* Returns have $h_{xy}(2) \approx 0.5$ (0.36–0.67), i.e., no long-range cross-correlation of the returns themselves. Absolute returns have $h_{xy}(2) = 0.78$–1.04, the long-memory volatility cross-correlations reported for the DJIA–NASDAQ pair in Ref. [3]. The median-detrended exponents of absolute returns exceed those of MF-X-DMA for 13 of the 16 pairs (median 0.97 versus 0.88).

(v) *Negative moments.* Cross fluctuation functions at negative q are dominated by segments in which the cross-covariance is close to zero or changes sign, and they scale poorly [Fig. 6(a)]. This affects every estimator; we therefore compare cross exponents of real data for $q \in [1, 4]$.

5.3 Sensitivity to data errors

As in Paper I, we inject data errors into the real returns and measure how much each estimator changes relative to its own clean value. This measures sensitivity, not accuracy. We consider the following errors:

- bad ticks (isolated misprinted prices) of 10σ or 50σ at 0.5% of the days, in one series or in both;
- erroneous returns of 10σ, which shift the price level permanently;
- microstructure noise of relative amplitude $\eta = 0.5$ on every log price.

A 50σ bad tick corresponds to a price misprinted by about 40%–70% for a typical index, the size of a misplaced decimal point in a low-priced stock. We compare Pearson's r, the DMCA coefficient ρ, the median-detrended $\rho_{1/2}$, the midhinge-detrended ρ_{mid} ($\lambda = 0.25/0.75$), the centered $\lambda = 0.25$ coefficient, and the first-order coefficients $\rho_{q=1}$ with moving-average and median trends. The sensitivity is the change of the coefficient averaged over scales, with three replicates per pair. The results are given in Table 7 and Figs. 7 and 8.

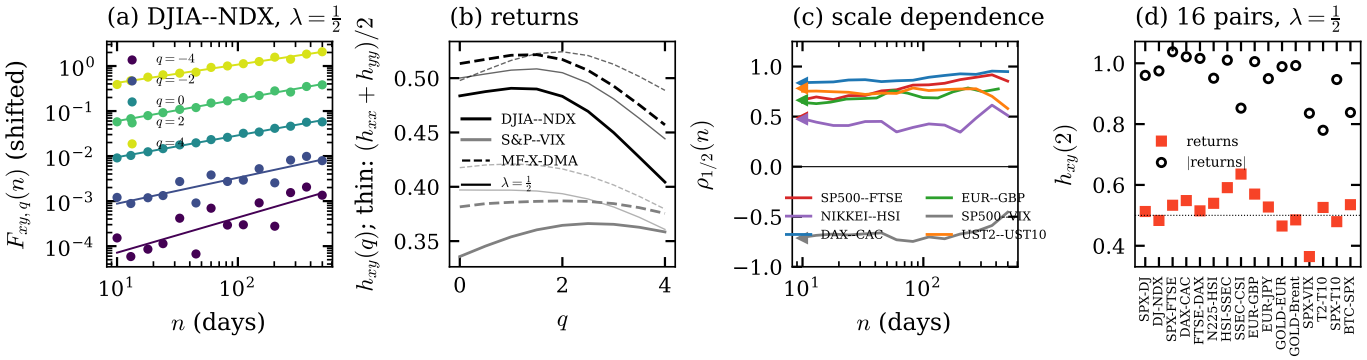


Figure 6: Financial cross-correlations. (a) $F_{xy,q}(n)$ of DJIA–NASDAQ-100 returns (MF-X-QDMA, $\lambda = 1/2$), shifted vertically; negative moments scale poorly. (b) $h_{xy}(q)$ for $q \geq 0$ (thick) and $[h_{xx} + h_{yy}]/2$ (thin) for two pairs and two estimators. (c) Median-detrended coefficient $\rho_{1/2}(n)$ for six pairs; triangles mark the daily Pearson coefficient. (d) $h_{xy}(2)$ of returns and of absolute returns for the 16 pairs.

Table 7: Sensitivity of correlation estimates of daily returns to injected data errors: median over pairs of the mean absolute change of the coefficient over scales ($\times 10^3$). Columns: Pearson r; DMCA ρ; median-detrended $\rho_{1/2}$; midhinge ρ_{mid}; centered $\lambda = 0.25$; first-order coefficients $\rho_{q=1}$ with moving-average and median trends. Last column: number of pairs for which $\rho_{1/2,q=1}$ is less sensitive than the DMCA coefficient. Bold: least sensitive detrended coefficient.

							$q=1$		
Error	Pairs	r	DMCA ρ	$\rho_{1/2}$	ρ_{mid}	$\rho_{0.25}$ c.	DMA	median	wins
Bad ticks in x, 10σ	16 pairs	165	11.4	10.7	11.5	21.6	9.6	**9.1**	13/16
	29 stocks	187	15.5	13.7	15.0	25.0	12.0	**11.5**	27/29
Bad ticks in x, 50σ	16 pairs	459	148.4	143.6	151.6	210.4	79.4	**77.2**	15/16
	29 stocks	517	173.9	165.7	175.0	227.6	98.5	**96.1**	29/29
Bad ticks in both, 10σ	16 pairs	288	25.0	22.9	24.8	44.0	**18.2**	18.9	12/16
	29 stocks	326	31.4	28.9	30.8	53.2	24.4	**23.4**	29/29
Bad ticks in both, 50σ	16 pairs	546	264.0	250.7	263.4	343.9	164.6	**155.0**	15/16
	29 stocks	628	286.1	269.1	283.1	361.8	182.1	**171.5**	29/29
Return outliers in x	16 pairs	108	122.3	132.0	125.0	144.9	**107.3**	108.6	10/16
	29 stocks	116	142.2	152.9	144.4	153.6	**130.7**	135.2	17/29
Microstructure noise	16 pairs	192	13.3	**13.0**	13.3	25.1	13.2	14.5	7/16
	29 stocks	210	16.5	**14.8**	16.5	27.7	17.3	17.6	5/29

The results separate into three regimes, which follow the mechanism identified in Paper I. A bad tick displaces a single profile value. An erroneous return shifts the profile permanently. Microstructure noise perturbs every profile value.

Bad ticks. Every detrended coefficient is far less sensitive than Pearson's r, because the detrended covariance spreads the error over many segments instead of concentrating it in one product. The median trend improves on the moving average consistently, but modestly. $\rho_{1/2}$ is less sensitive than the DMCA coefficient for 14–15 of the 16 pairs and 27–29 of the 29 stocks in every bad-tick scenario (Wilcoxon $p \leq 0.0013$), with a median ratio of 0.92–0.95. The larger gain comes from combining the median trend with first-order moments. Then $\rho_{1/2,q=1}$ is less sensitive than the DMCA coefficient for 12–15 of the 16 pairs ($p \leq 0.006$) and 27–29 of the 29 stocks ($p \leq 10^{-7}$), with a median ratio of 0.54–0.61 for 50σ errors and 0.72–0.76 for 10σ errors. Its sensitivity is 3.5–18 times smaller than that of r. Two mechanisms are at work. The quantile trend prevents an isolated error from biasing the trend in n windows (Paper I). The first-order moments limit the weight of the few segments that contain the error, which no trend can remove from the residual itself. For the cross exponents $h_{xy}(q \in [1,4])$, the median trend reduces sensitivity only for gross errors in both series (50σ: ratio 0.86–0.90; 27/29 stocks, $p = 5 \times 10^{-8}$; 14/16 pairs, $p = 0.003$). For 10σ errors there is no significant difference.

Erroneous returns. Quantile detrending does not help: $\rho_{1/2}$ is slightly *more* sensitive than the DMCA coefficient (ratio 1.07–1.08). Pearson's r, which sees each erroneous return only once, and the first-order coefficients are the least affected.

Microstructure noise. For the coefficient, the median is as good as the moving average or slightly better (ratio 0.94–1.00). For the cross exponents, the moving average is better (ratio of the median trend 1.17–1.47), as expected for dense Gaussian perturbations. The centered $\lambda = 0.25$ coefficient is the most sensitive detrended estimator in every regime (ratio 1.1–1.9 relative to DMCA), which is the price of removing the offset by centering. The midhinge is unbiased but no more robust than the moving average.

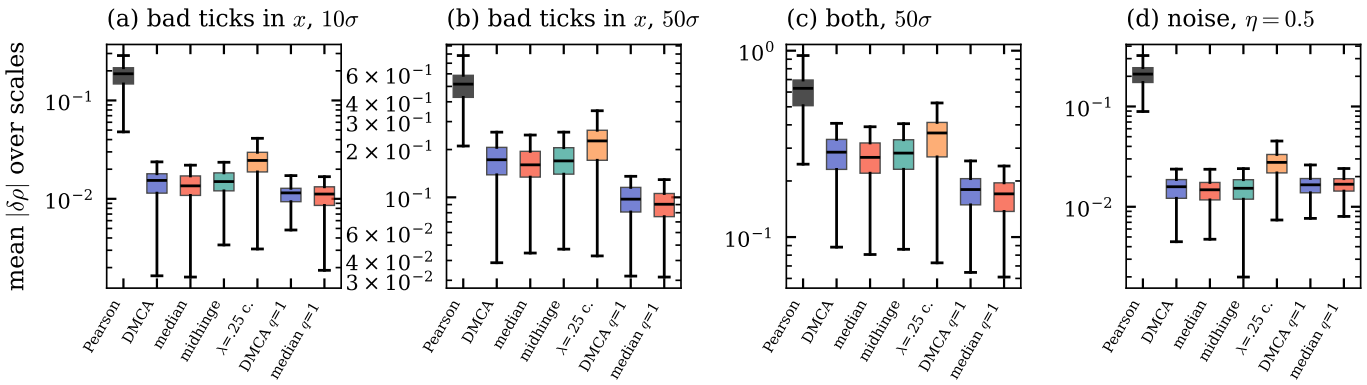


Figure 7: Sensitivity of correlation estimates of daily returns, distribution over the 16 financial pairs and the 29 DJIA stock–index pairs. (a), (b) 10σ and 50σ bad ticks at 0.5% of the days in one series. (c) 50σ bad ticks in both series. (d) Microstructure noise, $\eta = 0.5$. Labels: Pearson r; DMCA; $\lambda = 1/2$; midhinge; centered $\lambda = 0.25$; and the $q = 1$ coefficients with moving-average and median trends.

5.4 Time-varying correlations

Scale-resolved correlations are often tracked in rolling windows, for example to study contagion [26, 27] or the stock–bond relation [25]. We compute the coefficients at $n = 19$ days in four-year windows (1000 days, step 60 days), with and without 50σ bad ticks at 0.5% of the days of one series (Fig. 8). The clean S&P 500–Treasury coefficient changes sign in the window ending in April 2001, consistent with the literature [25]. The errors change the rolling Pearson coefficient by 0.27 on average, which is enough to mask the reversal. They change the DMCA coefficient by 0.16 and $\rho_{1/2,q=1}$ by 0.10. For DAX–CAC the corresponding changes are 0.63, 0.36, and 0.15. With $\rho_{1/2,q=1}$ the rolling correlation stays within about 0.15 of its clean value.

Table 8: Recommended use of MF-X-QDMA.

Situation	Recommendation
Measures	$\theta = 0$; mixed levels $(0.1, 0.9)$ or $(0.25, 0.75)$; no centering; reference exponents from the joint partition function [Eq. (10)], not the average rule.
Signals, coefficients	$\lambda = 1/2$ (or midhinge); avoid raw $\lambda \neq 1/2$ (Proposition 4).
Isolated data errors	$\rho_{1/2,q=1}$: median trend plus first-order moments.
Level-shifting errors	No benefit from quantiles; clean the data.
Dense noise	Moving average (MF-X-DMA).
Negative q	Unreliable when cross-covariances change sign; report $q > 0$.
Anticorrelation	Absolute convention for h_{xy}; sign from $\rho(n)$; or analyze $(x, -y)$ with $\lambda_y \to 1 - \lambda_y$.

6 Discussion

6.1 Practical guidelines

Table 8 collects the recommendations. For measures, the quantile levels are a free design choice: the mixed levels $(0.1, 0.9)$ gave the most accurate cross exponents. For signals, an offset-free trend is required, and the median is the natural choice. In both cases backward windows should be used, because the centered median is degenerate for measures (Corollary 2).

6.2 Limitations

(i) The advantage of mixed quantile levels for binomial pairs is empirical; we have no theory for its size. (ii) For monofractal signals MF-X-QDMA is not more accurate than the centered MF-X-DMA. (iii) The financial study uses daily data and synthetic errors injected into real returns. The magnitude of the gains in tick data, where bad prints are frequent [28, 29], remains to be established. (iv) The Bitcoin–S&P 500 pair is short ($N = 1375$), and its detrended coefficients (0.19 against $r = 0.03$) are dominated by a few heavy-tailed segments at large n; they should not be interpreted. (v) We have not studied partial cross-correlations [6], to which the quantile trend extends directly.

7 Conclusions

MF-X-QDMA extends quantile detrending to cross-correlations in one and two dimensions. For measures, it measures the joint partition function exactly. This gives exact cross exponents for cascade pairs and a Cauchy–Schwarz bound, which together show that the widely used average rule for cross exponents holds only for identical multipliers. For signals, quantile levels other than the median create spurious cross-correlation, which the median, the midhinge, or segment centering removes. Mixed quantile levels give the most accurate cross exponents of binomial pairs, and the quantile trend gives the most accurate exponents of 2D cascade pairs. In financial data, the median trend combined with first-order moments gives the scale-resolved correlation estimate that is least sensitive to isolated bad ticks: about half as sensitive as the DMCA coefficient for gross errors, and up to an order of magnitude less sensitive than Pearson's coefficient. It recovers

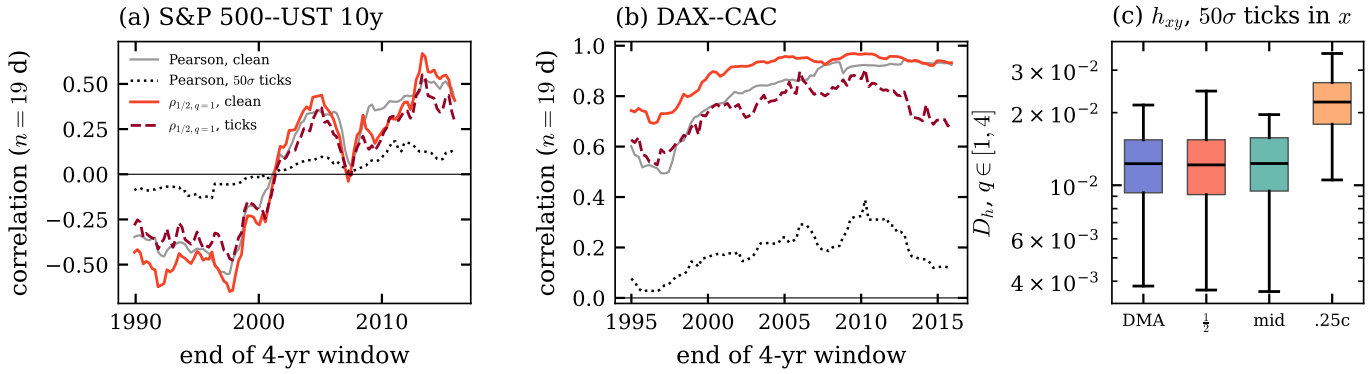


Figure 8: Time-varying correlations with and without 50σ bad ticks at 0.5% of the days of one series. (a) S&P 500–10-year Treasury and (b) DAX–CAC: Pearson coefficient and $\rho_{1/2,q=1}(n = 19)$ in four-year rolling windows. (c) Change of the cross exponents $h_{xy}(q \in [1,4])$ for 50σ bad ticks in x, over all 45 pairs.

the reversal of the stock–bond correlation under errors that mask it in the Pearson coefficient. Quantile detrending does not help against level-shifting errors or dense microstructure noise.

Acknowledgments

* Data availability. The financial series are from the public `qrmdata` collection [20]. The benchmark corpus, the code, and the numerical results underlying all tables and figures will be deposited in a public repository upon publication.

A Implementation

All residuals are computed as in Paper I. Moving quantiles at several levels are obtained from a single partial sort of each window, and 2D quantile trends from sliding views of the integral image. For a pair of series, the residuals of each series are computed once per scale and reused for every combination (λ_x, λ_y), for the auto fluctuation functions in Eq. (6), and for both moment conventions. For $N \approx 7000$ and 14 scales, MF-X-DMA, MF-X-QDMA at three levels, and MF-X-DFA together take about 0.7 s per pair on one CPU core.

References

[1] Boris Podobnik and H. Eugene Stanley. Detrended cross-correlation analysis: A new method for analyzing two nonstationary time series. *Phys. Rev. Lett.*, 100:084102, 2008.

[2] Wei-Xing Zhou. Multifractal detrended cross-correlation analysis for two nonstationary signals. *Phys. Rev. E*, 77: 066211, 2008.

[3] Zhi-Qiang Jiang and Wei-Xing Zhou. Multifractal detrending moving-average cross-correlation analysis. *Phys. Rev. E*, 84:016106, 2011.

[4] Paweł Oświęcimka, Stanisław Drożdż, Marcin Forczek, Stanisław Jadach, and Jarosław Kwapień. Detrended cross-correlation analysis consistently extended to multifractality. *Phys. Rev. E*, 89:023305, 2014.

[5] Jarosław Kwapień, Paweł Oświęcimka, and Stanisław Drożdż. Detrended fluctuation analysis made flexible to detect range of cross-correlated fluctuations. *Phys. Rev. E*, 92:052815, 2015.

[6] Xi-Yuan Qian, Ya-Min Liu, Zhi-Qiang Jiang, Boris Podobnik, Wei-Xing Zhou, and H. Eugene Stanley. Detrended partial cross-correlation analysis of two nonstationary time series influenced by common external forces. *Phys. Rev. E*, 91:062816, 2015.

[7] Gilney F. Zebende. DCCA cross-correlation coefficient: Quantifying level of cross-correlation. *Physica A*, 390: 614, 2011.

[8] Ladislav Kristoufek. Detrending moving-average cross-correlation coefficient: Measuring cross-correlations between non-stationary series. *Physica A*, 406:169, 2014.

[9] Boris Podobnik, Zhi-Qiang Jiang, Wei-Xing Zhou, and H. Eugene Stanley. Statistical tests for power-law cross-correlated processes. *Phys. Rev. E*, 84:066118, 2011.

[10] Zhi-Qiang Jiang, Wen-Jie Xie, Wei-Xing Zhou, and Didier Sornette. Multifractal analysis of financial markets: a review. *Rep. Prog. Phys.*, 82:125901, 2019.

[11] Sawon Pratiher. Quantile detrending moving average algorithm for multifractal time series and surfaces, 2026. companion paper, submitted jointly to Phys. Rev. E.

[12] Gao-Feng Gu and Wei-Xing Zhou. Detrending moving average algorithm for multifractals. *Phys. Rev. E*, 82: 011136, 2010.

[13] Roger Koenker and Gilbert Bassett. Regression quantiles. *Econometrica*, 46:33, 1978.

[14] Roger Koenker. *Quantile Regression*. Cambridge University Press, Cambridge, 2005.

[15] Rob J. Hyndman and Yanan Fan. Sample quantiles in statistical packages. *Am. Stat.*, 50:361, 1996.

[16] Frédéric Lavancier, Anne Philippe, and Donatas Surgailis. Covariance function of vector self-similar processes. *Stat. Probab. Lett.*, 79:2415, 2009.

[17] Robert B. Davies and David S. Harte. Tests for Hurst effect. *Biometrika*, 74:95, 1987.

[18] C. R. Dietrich and Garry N. Newsam. Fast and exact simulation of stationary Gaussian processes through circulant embedding of the covariance matrix. *SIAM J. Sci. Comput.*, 18:1088, 1997.

[19] J. R. M. Hosking. Fractional differencing. *Biometrika*, 68:165, 1981.

[20] Marius Hofert, Kurt Hornik, and Alexander J. McNeil. qrmdata: Data sets for quantitative risk management practice, 2025. R package version 2025-07-24-3, https://CRAN.R-project.org/package=qrmdata.

[21] Alexander J. McNeil, Rüdiger Frey, and Paul Embrechts. *Quantitative Risk Management: Concepts, Techniques and Tools*. Princeton University Press, Princeton, NJ, revised edition, 2015.

[22] Refet S. Gürkaynak, Brian Sack, and Jonathan H. Wright. The U.S. Treasury yield curve: 1961 to the present. *J. Monet. Econ.*, 54:2291, 2007.

[23] Thomas W. Epps. Comovements in stock prices in the very short run. *J. Am. Stat. Assoc.*, 74:291, 1979.

[24] Robert E. Whaley. The investor fear gauge. *J. Portfolio Manage.*, 26(3):12, 2000.

[25] Lieven Baele, Geert Bekaert, and Koen Inghelbrecht. The determinants of stock and bond return comovements. *Rev. Financ. Stud.*, 23:2374, 2010.

[26] François Longin and Bruno Solnik. Extreme correlation of international equity markets. *J. Finance*, 56:649, 2001.

[27] Kristin J. Forbes and Roberto Rigobon. No contagion, only interdependence: Measuring stock market comovements. *J. Finance*, 57:2223, 2002.

[28] Christian T. Brownlees and Giampiero M. Gallo. Financial econometric analysis at ultra-high frequency: Data handling concerns. *Comput. Stat. Data Anal.*, 51:2232, 2006.

[29] Ole E. Barndorff-Nielsen, Peter Reinhard Hansen, Asger Lunde, and Neil Shephard. Realized kernels in practice: trades and quotes. *Econom. J.*, 12:C1, 2009.